Power Electronic Systems
Laboratory

Proceedings of the 15th International Power Electronics and Motion Control Conference (ECCE Europe 2012), Novi Sad, Serbia, September 4-6, 2012

Hybrid Three-Phase Rectifier with Switched Current Injection Device

M. Jankovic,
M. Darijevic,
P. Pejovic,
J. W. Kolar,
Y. Nishida

Eidgenössische Technische Hochschule Zürich
Swiss Federal Institute of Technology Zurich

15th International Power Electronics and Motion Control Conference, EPE-PEMC 2012 ECCE Europe, Novi Sad, Serbia

Hybrid Three-Phase Rectifier with Switched Current Injection Device

M. Janković[1], M. Darijević[2], P. Pejović[3], J. W. Kolar[4], Y. Nishida[5]

[1]Faculty of Electrical Engineering, University of Belgrade, Serbia, marija18288@gmail.com
[2]Faculty of Electrical Engineering, University of Belgrade, Serbia, darijevic@gmail.com
[3]Faculty of Electrical Engineering, University of Belgrade, Serbia, peja@etf.rs
[4]Swiss Federal Institute of Technology, Zürich, Switzerland, kolar@lem.ee.ethz.ch
[5]Chiba Institute of Technology, Japan, nishida_yas@nifty.com

***Abstract* — A hybrid three-phase rectifier with switched current injection device and high frequency switching current injection network is analyzed in this paper. The rectifier applies suboptimal current injection. Optimization of the injected current amplitude is performed, resulting in the minimum of the input current THD of 4.36%. Ratings of applied semiconductor devices are derived. Effects caused by finite values of the inductance applied in the current injection network are analyzed. It is shown that increased values of the inductance require reduced amplitude of the injected current, and result in slightly increased values of the input current THD. A new structure of the current injection network that provides filtering of the switching ripple is proposed. The results are experimentally verified on a low-power converter model.**

***Keywords* — AC-DC power conversion, converters, harmonic distortion, power conversion harmonics, rectifiers.**

I. INTRODUCTION

In this paper, three-phase rectifiers that provide input currents with low content of higher order harmonics and good power factor applying switching current injection devices are analyzed. Basic structure of such rectifiers is proposed in [1] and [2], and in its generalized form it is shown in Fig. 1. Unless otherwise noted, constant output current is assumed. Basic part of the rectifier is a three-phase voltage supplied current loaded diode bridge (diodes D1 to D6), and it processes the main part of the rectifier power. To shape the input currents, a current injection system is applied, and it consists of a current injection device (switches S1 to S3), and a current injection network that provides currents i_{odd} and i_{even}. The theory behind the rectifier is given in [3], showing that it is possible to achieve purely sinusoidal input currents in phase with corresponding phase voltages by proper choice of i_{odd} and i_{even}. In that case, assuming that the dc component of i_{even} is zero, the current injection system takes about 9% of the rectifier input power. This power could be restored at the rectifier output through the dc component of i_{even}. Various structures to achieve this goal are presented in [3], most of them requiring only passive circuitry and/or low-frequency switching. Analysis shown in [3] also indicates that the biggest part of the input current shaping is done by the i_{odd} sources, and these sources also take the most of the power that should be restored through the dc component of i_{even}. In the case the ac component of i_{even} is omitted, it is shown that the input current total harmonic distortion (THD) of about 4% could be achieved, and this current injection method is named the suboptimal current injection. This method is a tradeoff where purely sinusoidal waveforms of the input currents are sacrificed, allowing distortion of about 4%, in order to simplify the current injection network.

An interesting current injection network is proposed in [4], resulting in the rectifier shown in Fig. 2. The rectifier of Fig. 2 requires high-frequency switching and significant filtering of the switching current ripple, but provides simultaneous injection of i_C and recovery of the power taken by i_C through the dc component of i_{even}. Unfortunately, the ac component of i_{even} is left out of control, thus the method can be classified as suboptimal current injection. Similar concept is applied in [5] for the rectifiers that apply magnetic current injection devices. In the area of inverters, the analyzed concept has been applied in [6]. In [7] and [8], the concept has been applied for supplying machine drives.

This paper is aimed as an extension of [4] both in

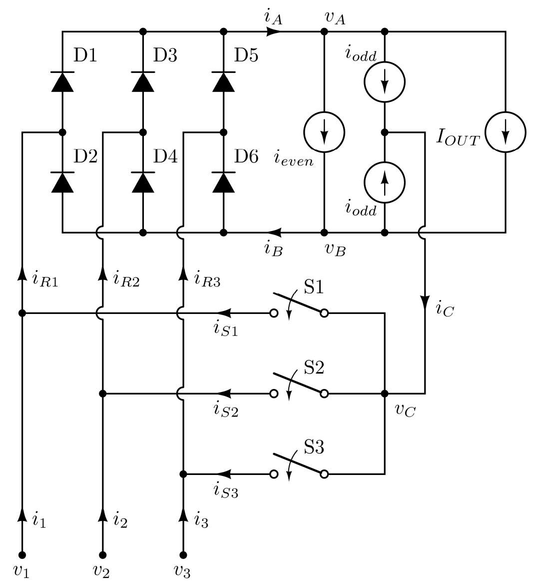

Fig. 1. Generic structure of a three-phase rectifier with switching current injection device.

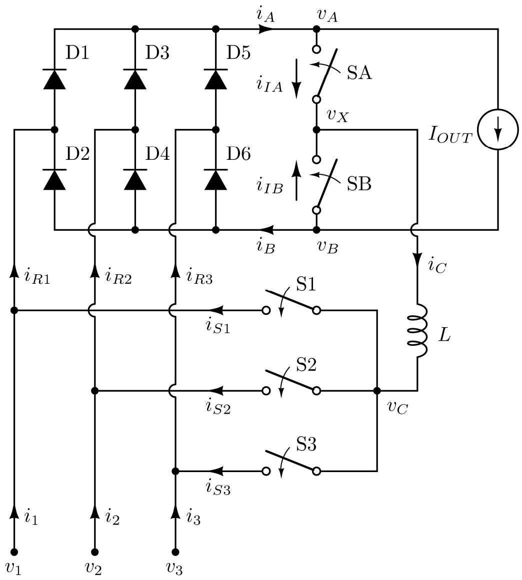

Fig. 2. Three-phase rectifier with switching current injection device and suboptimal current injection.

theoretical and application direction. Optimization of the injected current amplitude is performed, and ratings of applied semiconductor components are given in the case of the optimal injected current amplitude. Effects of finite inductance of the inductor applied to program the injected current are analyzed, and the optimization of the injected current amplitude is performed in this case, too. Finally, a current injection network that provides high-frequency filtering is proposed.

II. Structure and Operation of the Rectifier

The rectifier under analysis is presented in Fig. 2, and it consists of the three-phase diode bridge (D1 to D6), current injection device (S1, S2 and S3), and the current injection network consisted of the switches SA and SB and the inductor *L*. In the analysis, it will be assumed that the rectifier is supplied by a three-phase voltage system

$$v_k = V_m \cos\left(\omega t - (k-1)\frac{2\pi}{3}\right) \tag{1}$$

for $k \in \{1,2,3\}$, and that the diode bridge operates in the continuous conduction mode, resulting in

$$v_A = \max(v_1, v_2, v_3) \tag{2}$$

and

$$v_B = \min(v_1, v_2, v_3). \tag{3}$$

The switches in the current injection device (S1, S2, and S3) are operated such that the switch connected to the phase whose voltage is neither minimal nor maximal at a given time point is on, resulting in

$$v_C = -v_A - v_B. \tag{4}$$

Equations (2), (3), and (4) provide the waveforms of v_A, v_B, and v_C as stiff, not dependent on the currents involved with corresponding nodes.

To generalize the results of the analyses, normalization is performed. The voltages are normalized to the amplitude of the phase voltage, V_m, such that voltage $v(t)$ is normalized to $m(t)$ according to

$$m(t) = \frac{v(t)}{V_m} \tag{5}$$

while the currents are normalized to the output current, resulting in

$$j(t) = \frac{i(t)}{I_{OUT}}. \tag{6}$$

The switches SA and SB are operated such that the average value of i_C in normalized terms is given by

$$j_C = -g\, m_C. \tag{7}$$

In general, averaging over the switching period of SA and SB will be assumed in the paper, and it will not be explicitly underlined in the most part of the text that follows.

III. Optimization

To optimize the amplitude of the injected current, which reduces to finding the value of $g = g_{opt}$ that minimizes the input current THD, low inductance of the inductor in the current injection network will be assumed, $L \to 0$. In this case, average value of v_X is close to v_C. Since

$$\overline{m_X} = d\, m_A + (1-d) m_B \tag{8}$$

in normalized terms, where d is the duty ratio of SA, while $1-d$ is the duty ratio of SB ($\mathrm{SB} = \overline{\mathrm{SA}}$), and since it is assumed that $\overline{m_X} \approx m_C$, the duty ratio is given by

$$d = \frac{m_C - m_B}{m_A - m_B}. \tag{9}$$

The value of d is used to compute average values of the currents through SA and SB as

$$j_{IA} = \overline{j_{SA}} = d\, j_C \tag{10}$$

and

$$j_{IB} = \overline{j_{SB}} = (1-d) j_C. \tag{11}$$

The diode bridge load currents are given by $j_A = 1 + j_{IA}$ and $j_B = 1 - j_{IB}$, which is sufficient to construct the waveforms of the input currents knowing the states of the

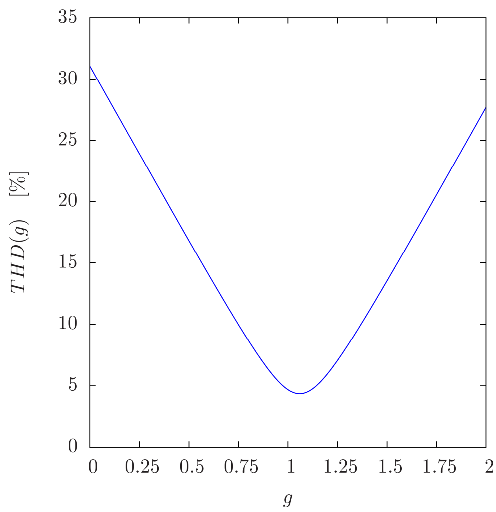

Fig. 3. Dependence of the input current *THD* on *g*.

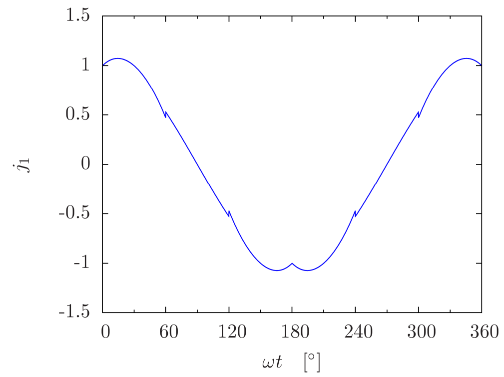

Fig. 4. Waveform of the input current j_1 for $g = g_{opt}$.

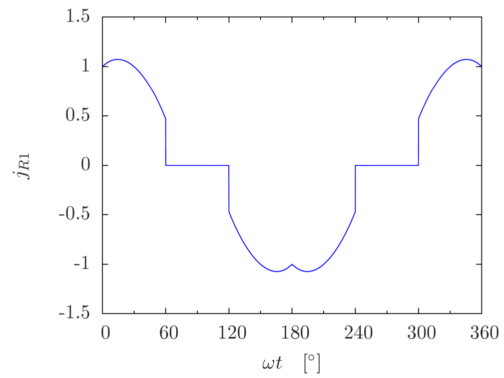

Fig. 5. Waveform of j_{R1} for $g = g_{opt}$.

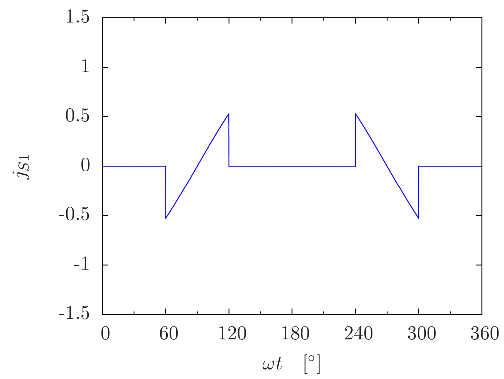

Fig. 6. Waveform of j_{S1} for $g = g_{opt}$.

diodes D1 to D6 and the switches S1 to S3.

Given equations and the inductor current programmed as specified by (7) result in dependence of the input current THD on g shown in Fig. 3. The minimum of $THD_{\min} = 4.36\%$ is reached for $g_{opt} = 1.0590$. Waveform of the input current that corresponds to this situation is given in Fig. 4, and corresponding waveforms of i_{R1} and i_{S1} are given in Figs. 5 and 6.

It is interesting to note here that changing the load type from the constant current load (I_{OUT}) to a constant power load (P_{OUT}) results in purely sinusoidal input currents for the choice of $g = 1.1010$. In this case, the output current ripple compensates for the missing i_{even} component. This case is of practical interest, since the constant power load

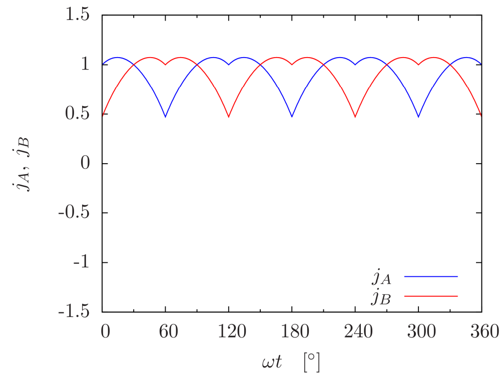

Fig. 7. Waveforms of j_A and j_B for $g = g_{opt}$.

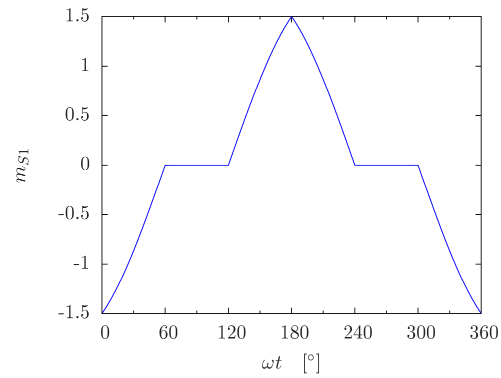

Fig. 8. Waveform of m_{S1} for $g = g_{opt}$.

is a good model for a dc-dc converter that might load the rectifier.

IV. Ratings of Semiconductor Components

Analyzing the waveforms obtained for $g = g_{opt}$, the power processed by the current injection system is found to be 5.54% of the input power. However, the power does not reflect the ratings of the semiconductor components: they are determined by the waveforms of corresponding voltages and currents, instead.

To determine the ratings of the diodes in the diode bridge, it should be noted that the reverse voltage applied across a diode is equal to the output voltage, having the maximal instantaneous value of $v_{OUT\max} = \sqrt{3}V_m$. Normalized waveforms of the averages of currents i_A and i_B , which are the currents that load the diode bridge, are given in Fig. 7, and their maxima are $j_{A\max} = j_{B\max} = 1.0735$. This means that in comparison to the rectifier without the current injection system, increase of the diode bridge maximum current is just 7.35%. Mean value of the diode bridge load currents, which is a parameter relevant to dimension low frequency rectifier diodes, is $\overline{j_A} = \overline{j_B} = 0.9136$, which means that in terms of average current the diode bridge is exposed to 91.36% of the load current.

To determine the ratings of the switches SA and SB, it should be noted that they are exposed to the same blocking voltage as the diodes of the diode bridge, having the maximum of $v_{OUT\max} = \sqrt{3}V_m$. Maximum value of the injected current i_C depends on parameter g, and for $g = g_{opt}$ it is $j_{C\max} = 0.5293$, meaning that the maximum of the current through the switches SA and SB is close to 53% of the output current.

To determine ratings of the switches in the current injection device, it should be noted that the waveform of the switch current is given in Fig. 6, having the maximum of about 53% of the output current, and the mean of the absolute value of 9% of the output current. Waveform of the voltage across S1 is given in Fig. 8, and it shows that the voltage applied across the switches is bipolar, having the maximum of the absolute value equal to $1.5\,V_m$, which is somewhat lower than the output voltage.

V. Effects of Finite Inductance Values

Results presented up to this point are obtained assuming negligible value of L. This assumption should be analyzed, since the inductance would have some finite value. Influence of the finite value of L is observed in the waveform of v_X

$$v_X = v_C + L\frac{d\,i_C}{d\,t}\,. \tag{12}$$

In normalized terms this reduces to

$$m_X = m_C + \frac{\omega L}{V_m} I_{OUT} \frac{d\,j_C}{d\,\omega t} \tag{13}$$

and introducing

$$x_l = \frac{\omega L}{V_m} I_{OUT} \tag{14}$$

having in mind $j_C = -g\,m_C$, m_X is obtained as

$$m_X = m_C - x_l\,g\frac{d\,m_C}{d\,\omega t}\,. \tag{15}$$

After the waveform of m_X is determined, actual value of d is given by

$$d = \frac{m_X - m_B}{m_A - m_B} \tag{16}$$

and the optimization is repeated for a set of values for x_l ranging from 0 to 0.5. Increased values of x_l correspond to reduced values of g_{opt}, as shown in Fig. 9. Dependence of $THD_{\min}$ on x_l is given in Fig. 10, illustrating slight increase of $THD_{\min}$ with x_l.

Waveform of j_1 which corresponds to $x_l = 0.5$, $g_{opt} = 0.9239$, and $THD_{\min} = 9.33\%$ is presented in Fig. 11.

VI. Filtering

An important issue in the proposed rectifier topology is filtering of the switching current ripple. The problem is pronounced since the currents taken by the current injection system are discontinuous if pre-filtering of i_{IA} and i_{IB} was not applied. To provide such pre-filtering, a current injection network shown in Fig. 12 is proposed. The circuit of Fig. 12 replaces SA, SB and L in the circuit

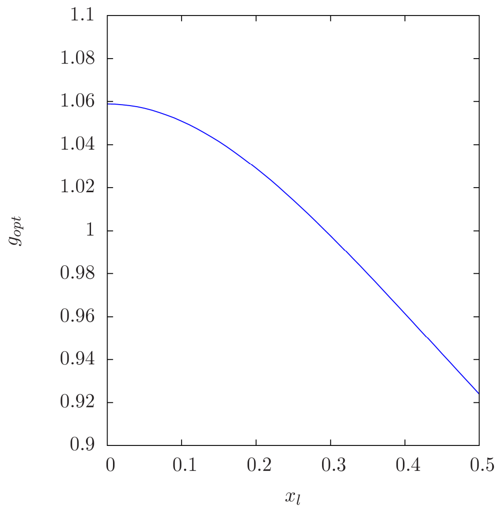

Fig. 9. Dependence of g_{opt} on x_l.

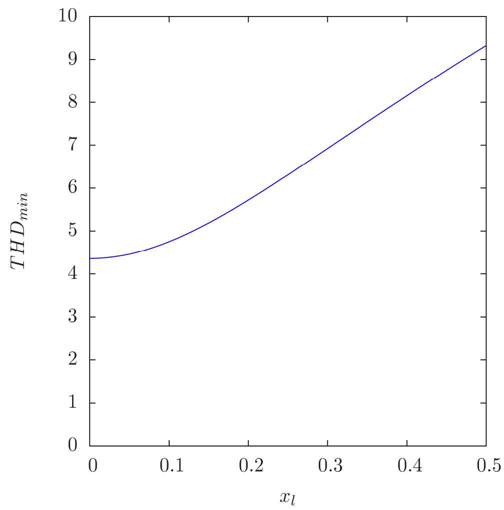

Fig. 10. Dependence of $THD_{\min}$ on x_l.

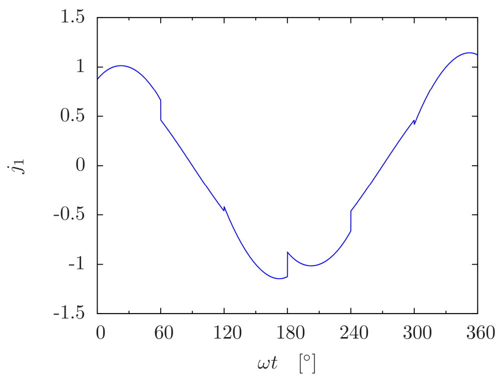

Fig. 11. Waveform of the input current j_1 for $x_l = 0.5$.

of Fig. 2. In this manner, continuous currents i_{IA} and i_{IB} are provided, instead of the discontinuous i_{SA} and i_{SB}. It would be ideal to provide $i_{IA} = \overline{i_{SA}}$ and $i_{IB} = \overline{i_{SB}}$. However, this is not possible due to the low-frequency ringing components of currents through the filtering

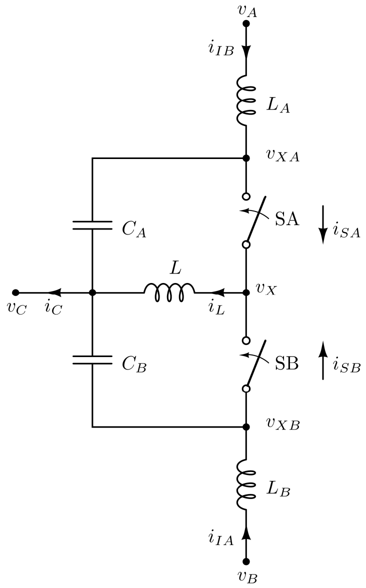

Fig. 12. Current injection network with filtering.

elements $L_A = L_B$ and $C_A = C_B$. Thus, the filter design is a compromise between an efficient high-frequency filtering and reducing the low-frequency ringing currents.

To design the filter, spectra of the currents intended to be filtered are of interest. A numerically efficient method to determine spectra is developed to perform this task. The method is based on a quasi steady state approximation, which separates high frequency processes in the circuit from the low frequency processes. For the analysis of high frequency processes, the low frequency processes are assumed constant in time, and the circuit is assumed to operate in the steady state. In this manner, amplitude of the switching ripple and the waveforms inside a switching interval are obtained, while the mean values of the waveforms remained unknown. On the other hand, to analyze low frequency processes, the circuit averaging is performed, and the simulation provided waveforms of the voltages and currents averaged over the switching period, being free of the switching ripple. To determine required spectra, actual waveforms are constructed by adding properly scaled ripple waveforms to the average values obtained analyzing the averaged circuit.

To illustrate the method, waveform of j_L is presented in Fig. 13, having the switching frequency to the line frequency ratio as high as 1024. Amplitude of the switching ripple is allowed to be 20% of the inductor maximum current. Just to provide an illustration, spectrum of j_{SA} is presented in Fig. 14, containing typical spectral groups around multiples of the switching frequency. Removal of these spectral groups is the ask of the filtering components, L_A, L_B, C_A and C_B.

VII. Experimental Results

To verify the analytically obtained results, an experimental setup is built. Due to the lab limitations, the input three-phase voltages are chosen to be with 24 V of the rms value, and the rated power of the experimental setup was about 250W. Such a low power setup is used just to prove the concept proposed in the paper. The ac side parameters measured at the experimental rectifier are given in Table I. The numerical values are obtained by offline digital signal processing of the waveforms recorded by the digital oscilloscope.

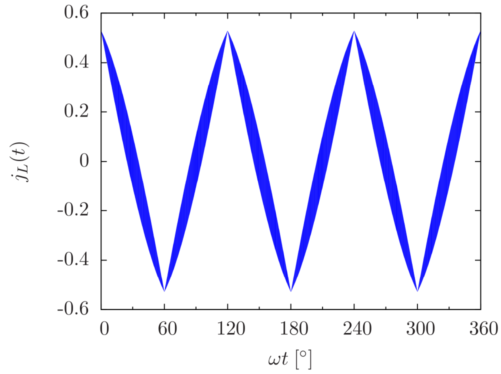

Fig. 13. Waveform of j_L.

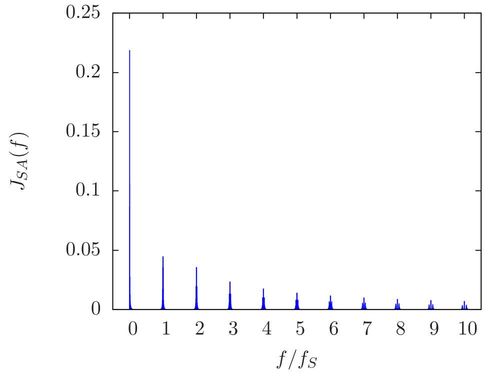

Fig. 14. Spectrum of j_{SA}.

TABLE I: EXPERIMENTAL RESULTS: AC SIDE DATA

phase, k	1	2	3
V_m [V]	27.6	27.8	27.8
I_m [A]	6.40	6.44	6.48
$THD(i_k)$ [%]	3.95	3.74	3.96
$THD(v_k)$ [%]	5.16	4.33	4.95
PF	0.976	0.983	0.985

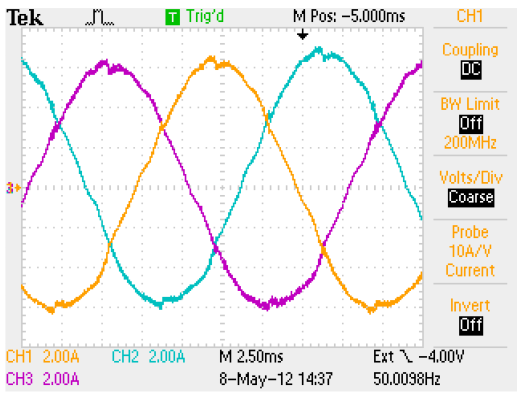

Fig. 15. Phase currents for $I_{OUT} = 5$ A and $V_{OUT} = 45$ V.

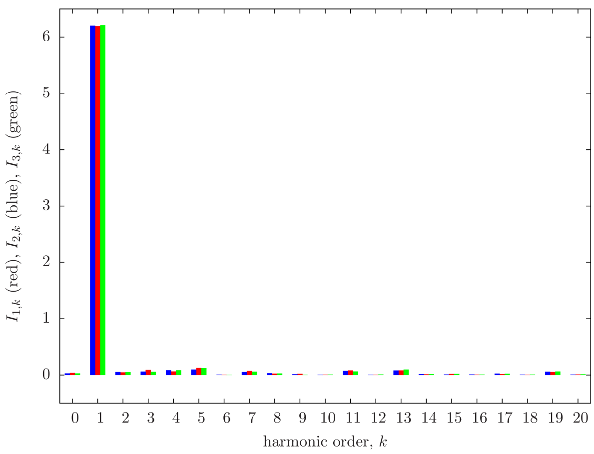

Fig. 16. Spectra of the phase currents.

To program i_C to be proportional to v_C, hysteresis window current mode control is applied. In this manner suboptimal current injection is implemented. In Fig. 15, waveforms of the input currents are presented. The waveforms are close to sinusoidal, symmetrical, and in a good agreement with the theoretical predictions. Amplitude spectra of the input currents are given in Fig. 16, showing low harmonic content of the waveforms, in accordance with the THD values provided in Table I.

Waveforms of i_{R1}, $-i_{S1}$ and i_1 are given in Fig. 17 to illustrate the current injection process and operation of the switching current injection device. The switching current injection device provided injection of the current i_C to the phase whose voltage is neither minimal nor maximal at the considered time interval, resulting in reverse bias of the diodes connected to the phase. This results in the gaps in the input currents of the diode bridge, i_{Rk}, $k \in \{1,2,3\}$, being patched by the current injection device currents $-i_{Sk}$. The waveform of $-i_{Sk}$ is given in the second diagram of Fig. 17, and it patches the gaps in i_{R1}. Waveform of i_1 is given in the last diagram of Fig. 17, and its close to sinusoidal waveform is obtained as a sum of i_{R1} and $-i_{S1}$. In this manner, $-i_{S1}$ successfully patched the gaps in i_{R1} due to the operation of the switching current injection device which directs i_C to a phase where current patching is needed.

Waveforms of the load currents of the diode bridge, i_A and i_B, are given in Fig. 18. The experimentally obtained currents are in a good agreement with the theoretically predicted waveforms given in Fig 7.

In Fig. 19, waveforms of i_A and i_{IA} are presented, showing that the dc component of i_A is transferred to the load, while the ac component forms i_{IA}, which later on forms a part of i_C.

The output voltage and the output current, which consists of the dc component only, are given in Fig. 20, being in complete agreement with the theoretical expectations.

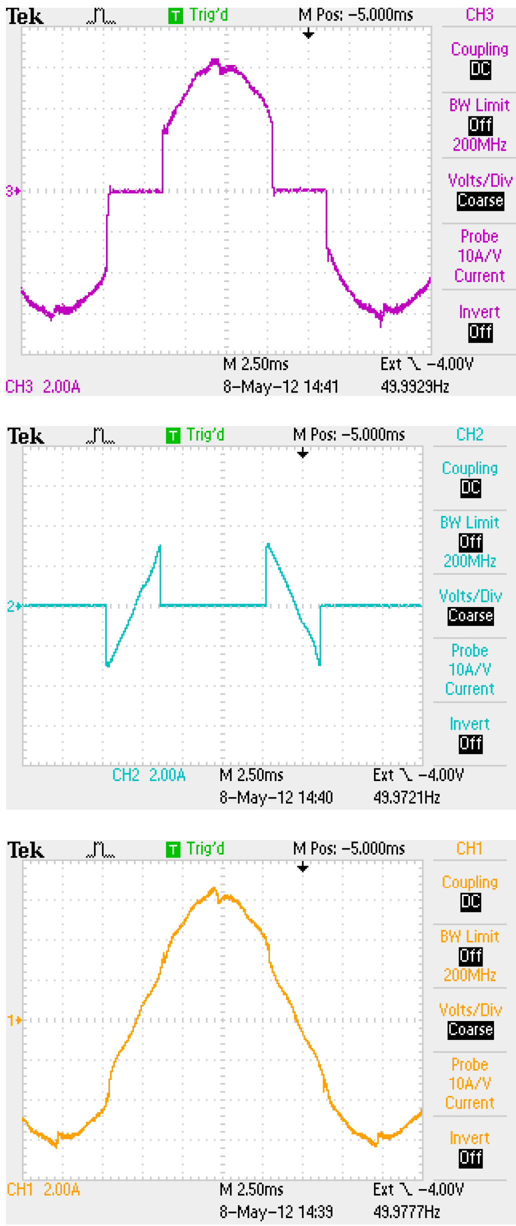

Fig. 17. Waveforms of i_{R1}, $-i_{S1}$, and i_1.

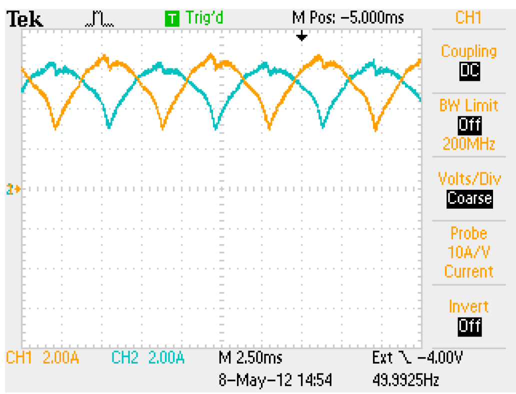

Fig. 18. Waveforms of i_A and i_B.

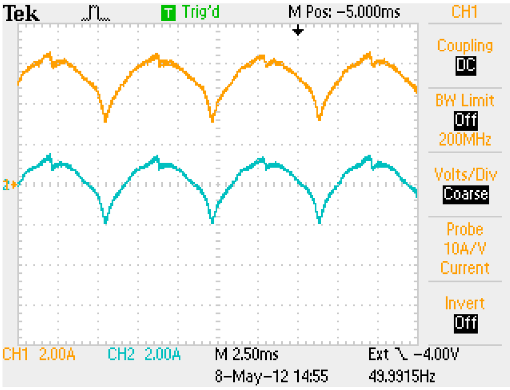

Fig. 19. Waveforms of i_A and i_{IA} .

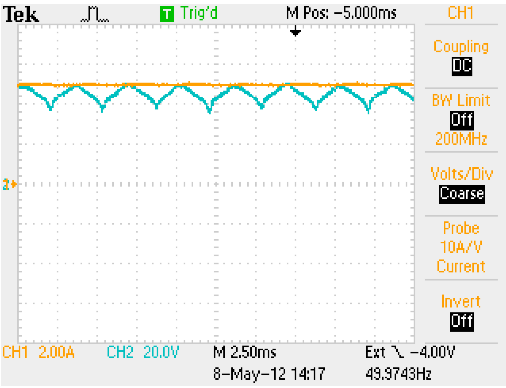

Fig. 20. Waveforms i_{OUT} and v_{OUT} .

VIII. Conclusion

A hybrid three-phase rectifier with switched current injection device and high frequency switching the current injection network is analyzed in this paper. The rectifier structure that applies suboptimal current injection is introduced, and optimization of the injected current amplitude in order to minimize THD of the input currents is performed. Minimum of $THD = 4.36\%$ is reached for the constant curret load, while $THD = 0$ could be achieved for the constant power load. For the optimal value of the injected current amplitude, ratings of applied semiconductor devices are derived and analyzed. The analysis indicates moderate requests imposed to the switching devices. Effects caused by finite values of the inductance of the inductor applied in the current injection network are analyzed next. It is shown that increased values of the inductance require reduced amplitude of the injected current and result in slightly increased values of the input current THD. Filtering of the currents in the current injection system is analyzed next, and a new structure of the current injection network that provides filtering is proposed. A novel numerically efficient method to compute spectra of the high frequency switched currents is developed and applied to estimate the spectra of the currents to be filtered. To verify the proposed concept, a low power and low voltage experimental rectifier model is built. The model is supplied with three-phase voltage system of only 24 V in rms value, having the rated power of 250 W. Regardless the low voltages and the low power, the rectifier model provided the experimental results in agreement with the theoretical predictions and successfully verified feasibility of the proposed rectifier concept.

References

[1] P. Pejović, "Low Harmonic Three Phase Rectifier," *Power Electronics Specialists Conference*, Galway, June 2000, pp. 1029–1034

[2] P. Pejović, "A Novel Low Harmonic Three Phase Rectifier," *IEEE Transactions on Circuits and Systems I: Fundamental Theory and Applications*, vol. 49, no. 7, pp. 955–965, July 2002.

[3] P. Pejović, *Three-Phase Diode Rectifiers with Low Harmonics—Current Injection Methods*, Springer, 2007.

[4] N. Vázquez, H. Rodriguez, C. Hernández, E. Rodríguez, J. Arau, "Three-Phase Rectifier With Active Current Injection and High Efficiency," *IEEE Transactions on Industrial Electronics*, vol. 56, no. 1, Jan. 2009, pp. 110–119.

[5] J.-I. Itoh, I. Ashida, "A Novel Three-Phase PFC Rectifier Using a Harmonic Current Injection Method," *IEEE Transactions on Power Electronics*, vol. 23, no. 2, Mar. 2008, pp. 715–722.

[6] M. Jantsch, C. W. G. Verhoeve, "Inverters with three-phase output and without electrolyte capacitor for improved lifetime," in *Proc. 14th European Photovoltaic Solar Energy Conf. and Exhibition EU PVSEC '97*, June 30—July 04, 1997, pp. 1–3.

[7] H. Yoo, S. K. Sul, "A novel approach to reduce line harmonic current for a three-phase diode rectifier-fed electrolytic capacitor-less inverter," in *Proc. 24th Annual IEEE Applied Power Electronics Conference and Exposition* (*APEC*), Feb. 15–19, 209, pp. 1897–1903.

[8] H. Yoo, S. K. Sul, "A new circuit design and control to reduce input harmonic current for a three-phase ac machine drive system having a very small dc-link capacitor," in *Proc. 25th Annual IEEE Applied Power Electronics Conference and Exposition* (*APEC*), Feb. 21–25, 2010, pp. 611–618.